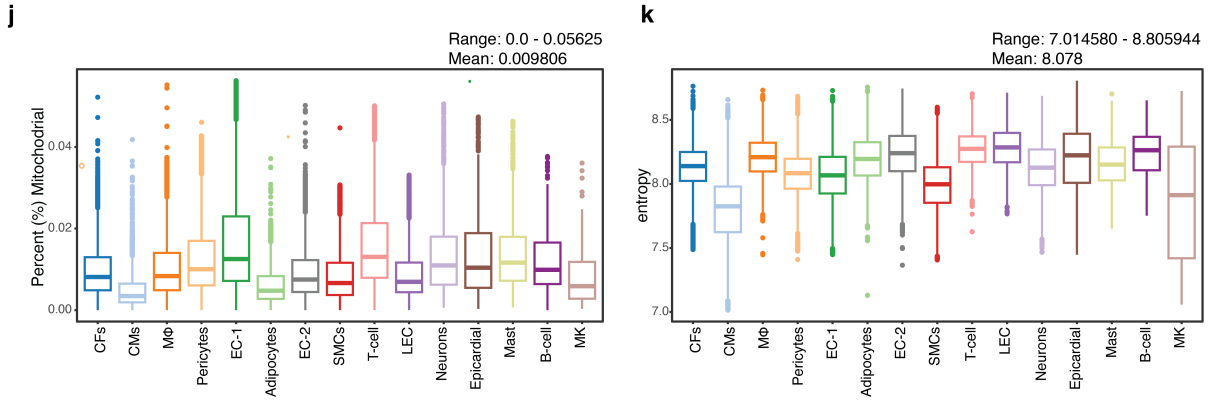
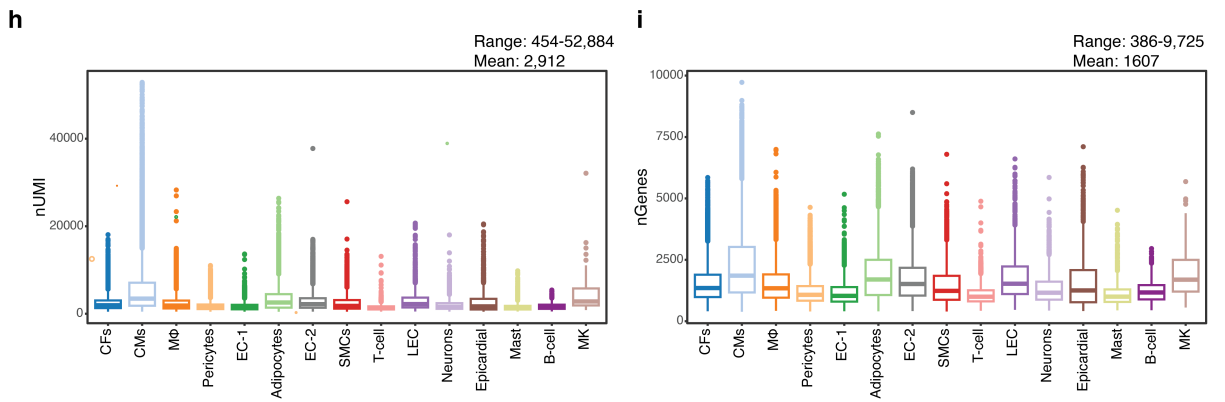
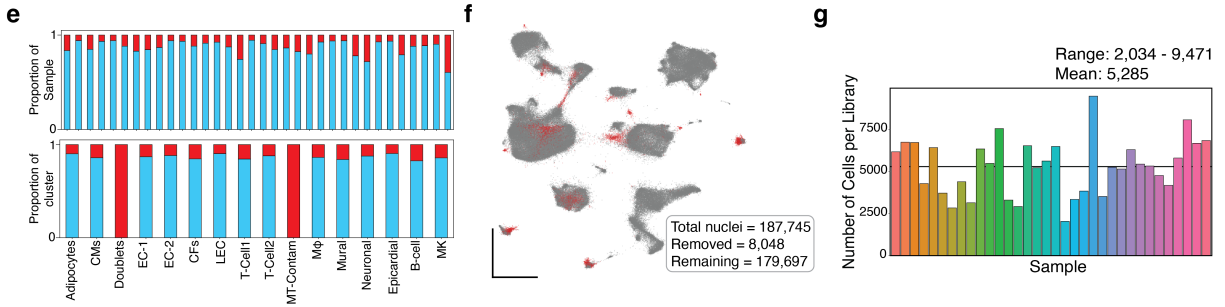
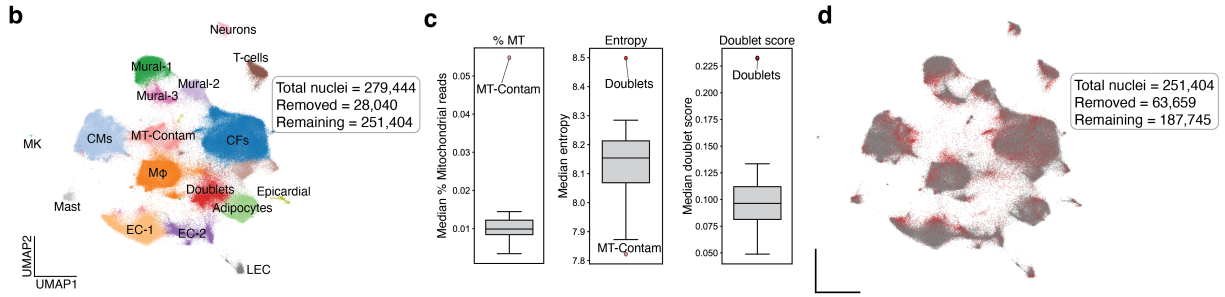
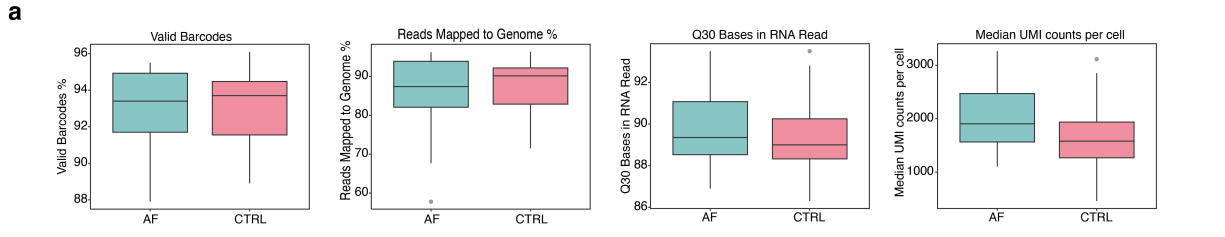


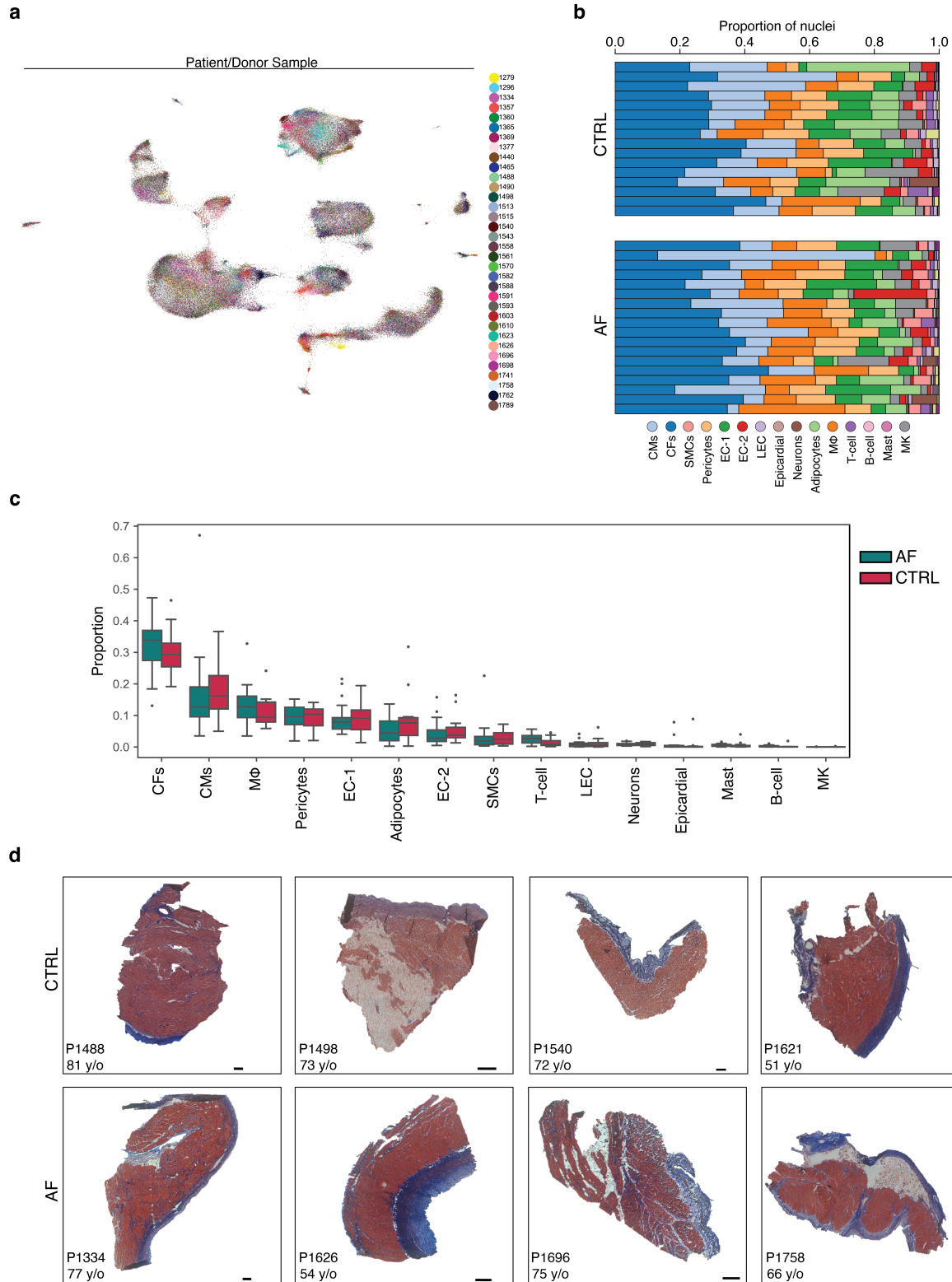
Supplementary Information

Large-scale Single-nuclei Profiling Identifies Role for *ATRNL1* in Atrial Fibrillation

Matthew C. Hill^{1,2,*}, Bridget Simonson^{1,*}, Carolina Roselli^{1,*}, Ling Xiao^{1,2}, Caroline Herndon¹, Mark Chaffin,¹ Helene Mantineo¹, Ondine Atwa¹, Harshit Bhasin¹, Yasmine Guedira¹, Kenneth C. Bedi Jr.³, Kenneth B. Margulies³, Nathan R. Tucker⁴, and Patrick T. Ellinor^{1,2}

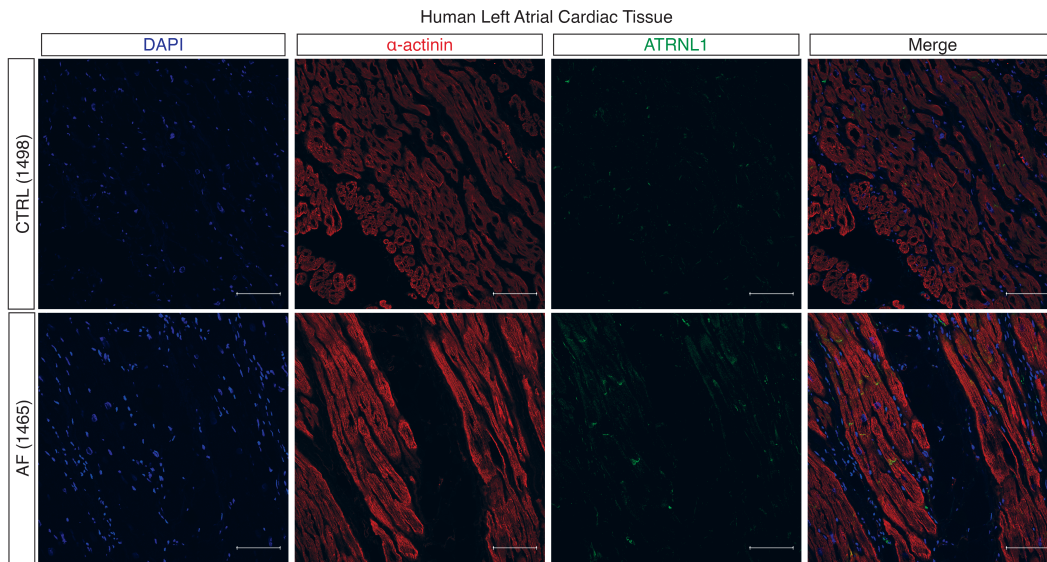
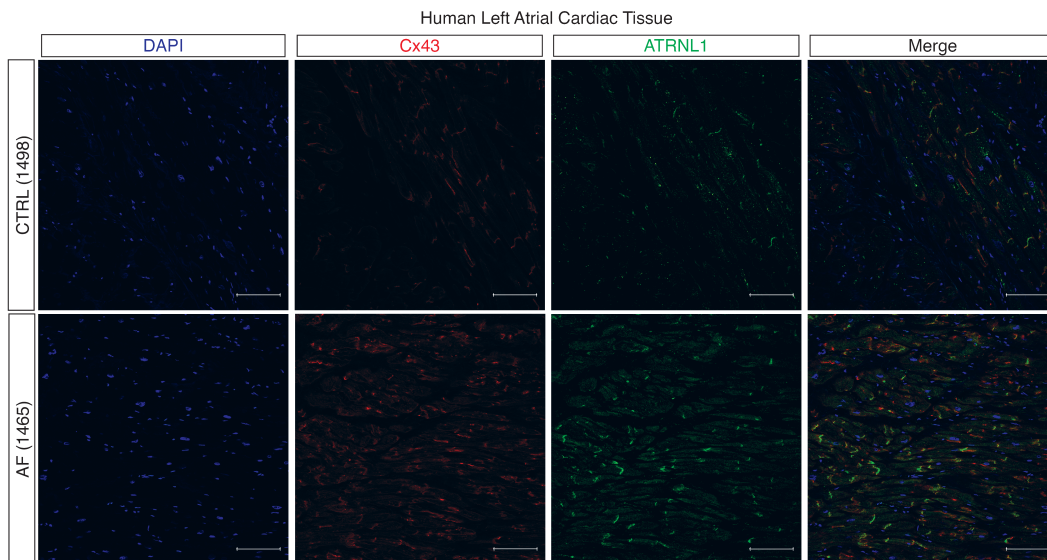
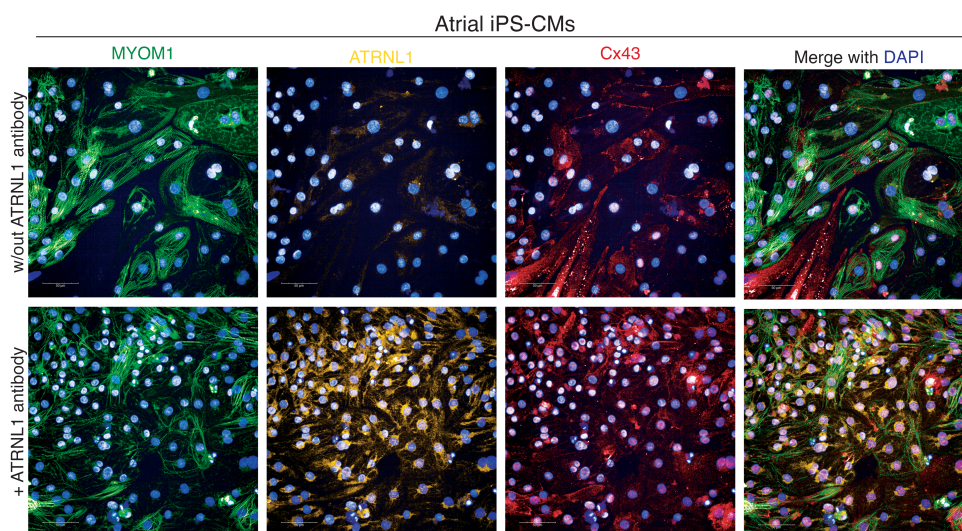


Supplemental Figure 1. snRNA-seq sample quality control metrics. **a** Distribution of snRNA-seq quality control metrics for each library derived from CellRanger count as box plots grouped by patient category. **b** UMAP embedding of all nuclei post-sample QC (n = 279,444) colored by Leiden clustering and labelled according to predicted cell type. **c** Distribution of the median of three quality control metrics for each cluster shown as boxplots, including percent of unique molecular identifiers (UMIs) mapping to mitochondrial genes (% MT), entropy, and the Scrublet estimated doublet score. Clusters containing cells to be removed are highlighted in red (n= 28,040 nuclei). **d** UMAP embedding of all nuclei after removal of low-quality clusters identified in **b** and **c** (n = 251,404). Additional low-quality nuclei as detected per cluster and per-sample are colored in red. **e** Proportion of each sample and cluster removed during the quality control procedure shown as stacked bar graph. **f** UMAP representation of remaining nuclei after removal of low-quality clusters and per-cluster quality control. Red nuclei were deemed as misclassified or low-quality following sub-cluster analysis. **g** Number of nuclei per library included in final snRNA-seq embedding. **h** Distribution of number of unique molecular identifiers (nUMI). **i** Distribution of number of unique genes (nGene). **j** Distribution of percentage of mitochondrial transcripts per cell. **k** Distribution of entropy across nuclei of each unique cell type. Center line, median; box limits, upper and lower quartiles; whiskers, 1.5x interquartile range.



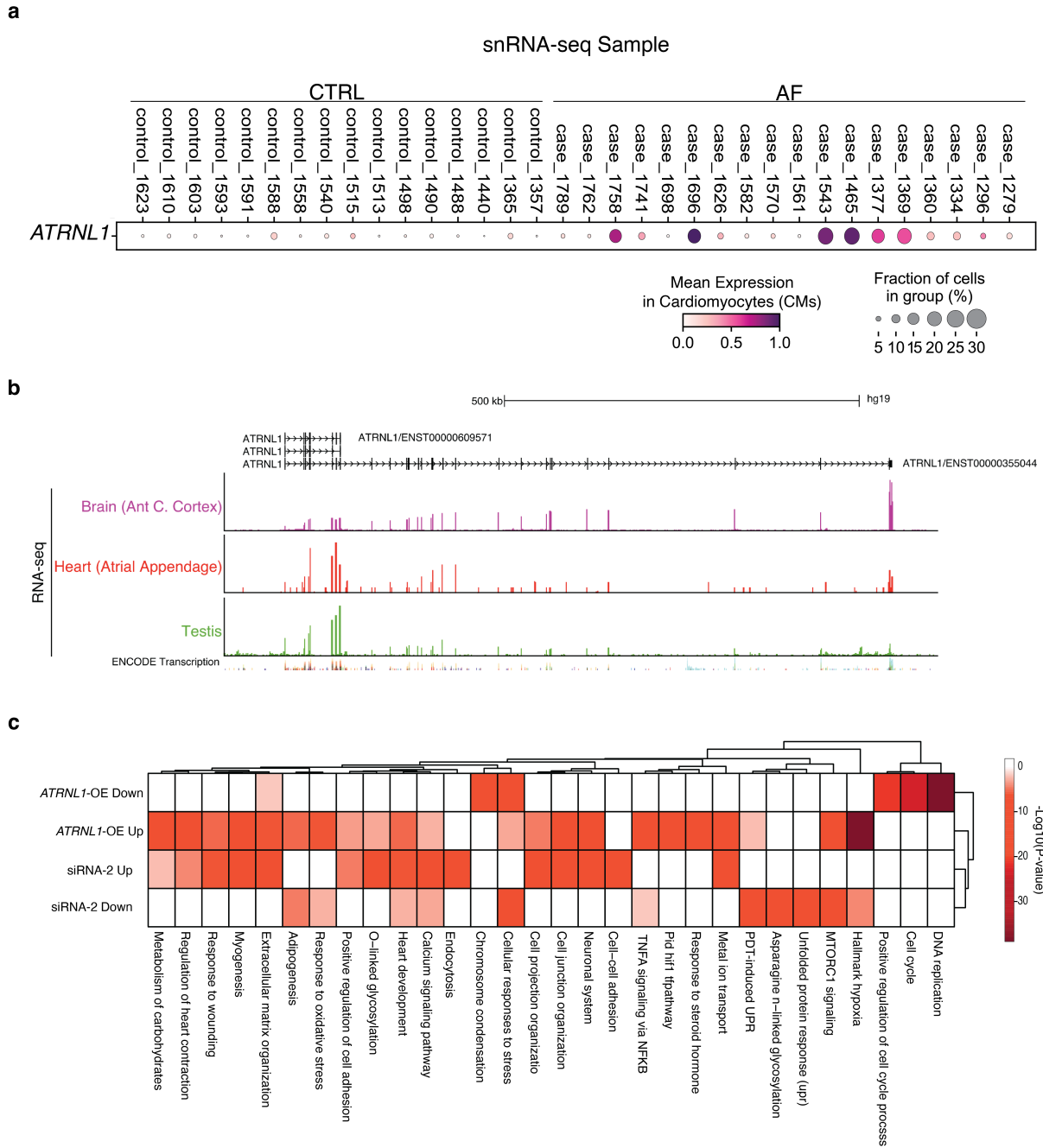
Supplemental Figure 2. Cellular composition of non-AF and AF patients LA tissue. **a** UMAP embedding of 179,697 cardiac nuclei colored by patient sample ID. **b** Cell-type composition of each individual human sample with cell-type colored according to our cluster annotations. **c** Box plot displaying the differences in cell composition

calculated with ScCODA for each cardiac cell type in controls (red) and patients with atrial fibrillation (AF) (blue). Boxplot represented as: center line, median; box limits, upper and lower quartiles; whiskers, 1.5x interquartile range; points, outliers. **d** Mason's trichrome staining of LA samples from patients included in snRNA-seq analysis.

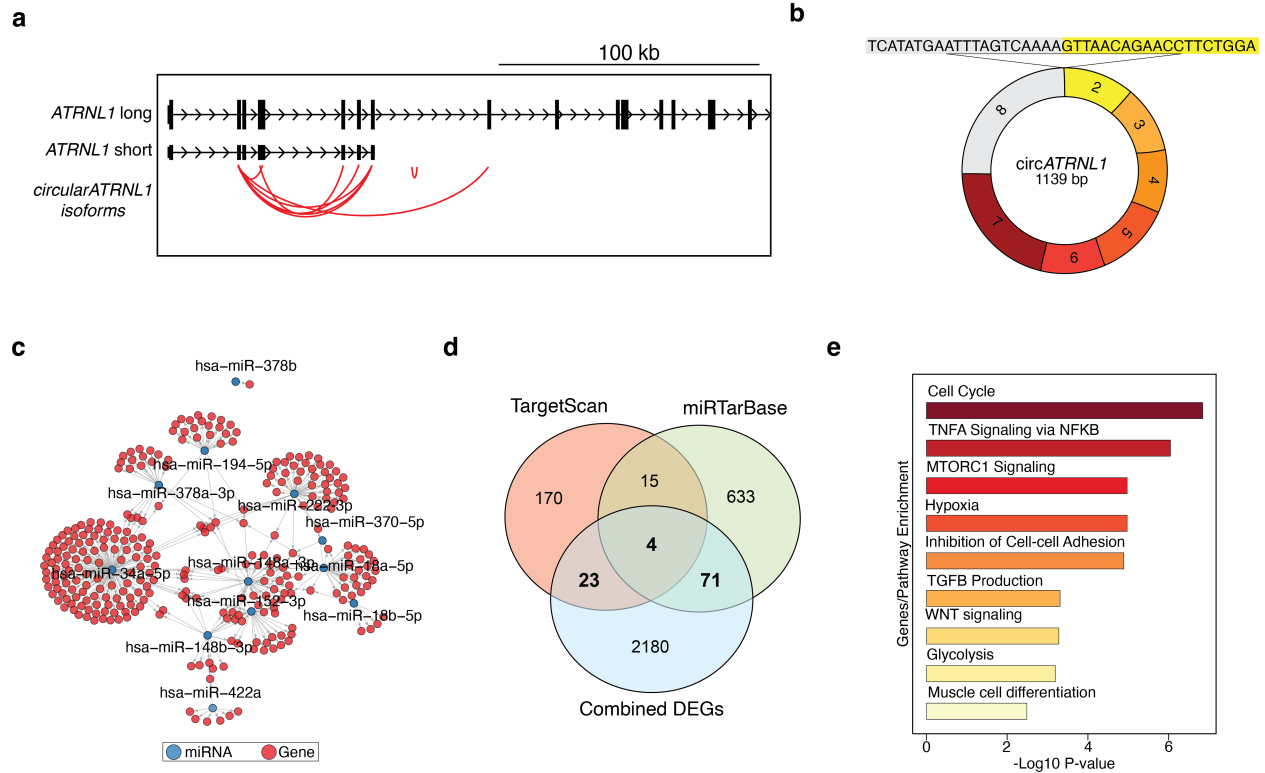
a**b****c**

Supplemental Figure 3. Subcellular localization of ATRNL1 in human LA tissue. a Tissue immunohistochemistry for nuclei/DAPI (blue), α -actinin (red), and ATRNL1 (green) in control and AF LA tissue. **b** Tissue immunohistochemistry for nuclei/DAPI (blue), Cx43 (red), and ATRNL1 (green) in control and AF LA tissue. Scale bars = 100 μ m. **c** Immunohistochemistry for nuclei/DAPI (blue), MYOM1 (green), Cx43 (red), and ATRNL1 (gold) in hESC-aCMs. Scale bars = 50 μ m.

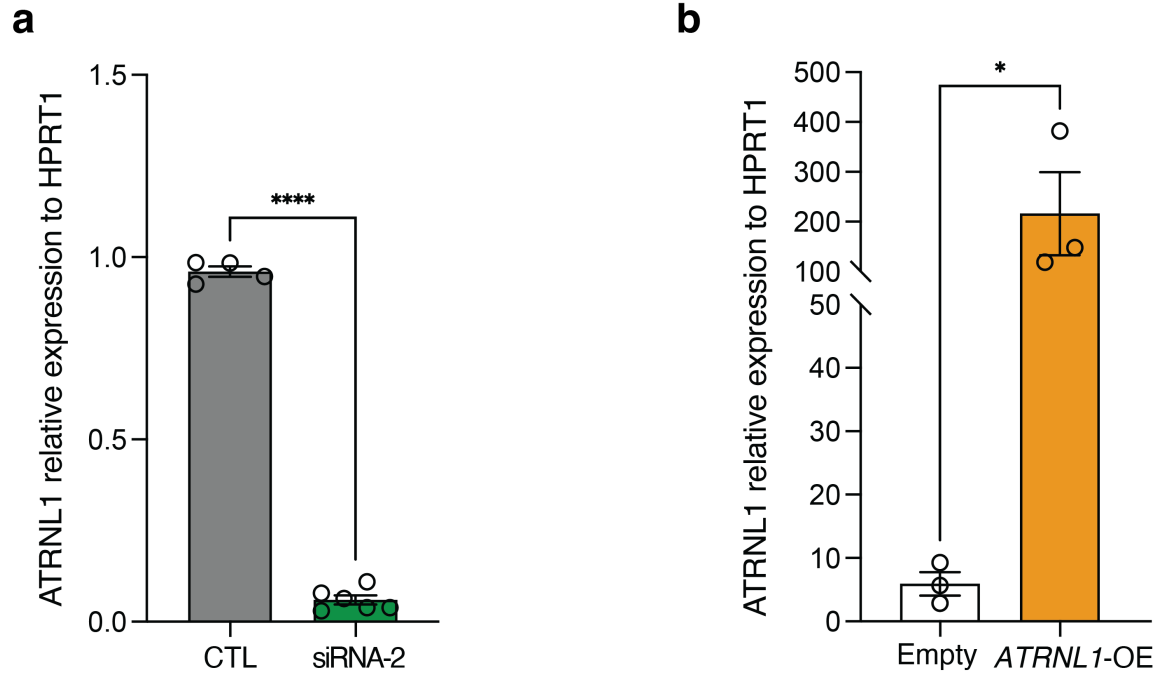
Supplemental Figure 4. Tissue expression of ATRNL1. **a** UMAP embedding of Human Heart Cell Atlas colored by cell state. **b** Dot plot showing expression of *ATRNL1* across all common cardiac cell states (non-immune cells). **c** Immunostaining of human left ventricular (LV) tissue. **d** Immunostaining of human left ventricular (LV) tissue and left atrial (LA) tissue controlling for primary antibody. Samples treated stained with DAPI and secondary antibodies only.



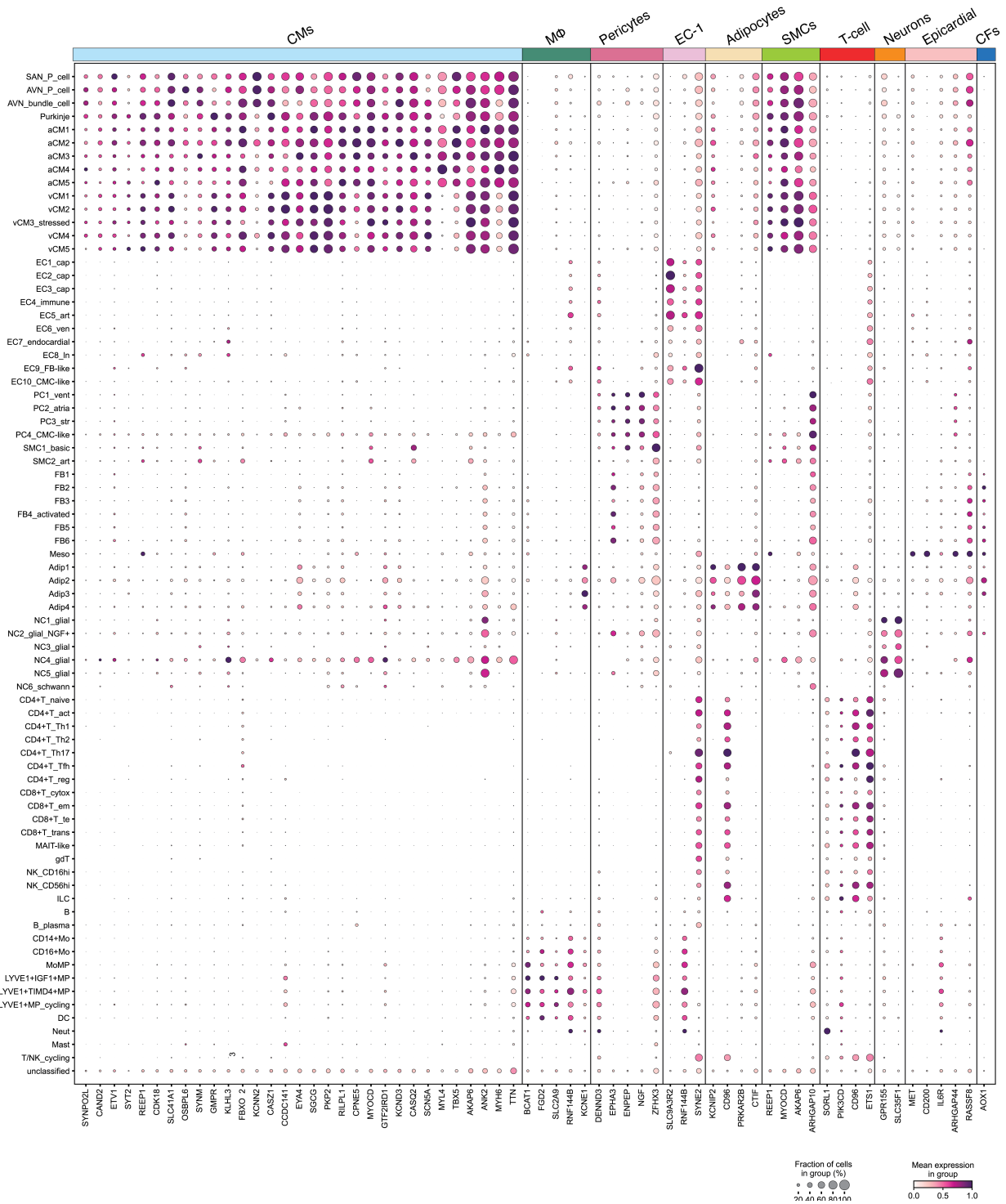
Supplemental Figure 5. Transcriptional profiling of hESC-aCMs. **a** Dot plot displaying the expression of *ATRNL1* in cardiomyocytes across all samples. **b** Genome browser tracks displaying GTEx RNA-seq reads mapped to the human genome (hg38). **c** Heatmap displaying pathway analysis colored by significance of enrichment ($-\text{Log}_{10}$ P-value). Differentially expressed genes from the indicated conditions were used for pathway enrichment analysis.



Supplemental Figure 6. Circular *ATRNL1* isoforms in hESC-aCMs . a Genome browser tracks displaying detectable *circATRNL1* isoforms uncovered from our total RNA-seq analysis in human hESC-aCMs (hg38). **b** Diagram of the most common *circATRNL1* isoform detected in hESC-aCMs. **c** Target gene prediction network of miRNAs with significant binding scores to *circATRNL1*. **d** Venn diagram displaying the intersection of TargetScan, miRTarBase with the combined differentially expressed genes identified in **Fig. 5h**. **e** Pathway enrichment analysis for all 98 common genes identified in **Supplemental Fig. 6d**.



Supplemental Figure 7. Manipulation of *ATRNL1* levels in hESC-aCMs. **a** qPCR results of *ATRNL1* knockdown in hESC-aCMs with siRNA-2. **b** qPCR results of *ATRNL1* overexpression in hESC-aCMs transduced with a lentiviral *ATRNL1*-OE vector.



Supplemental Figure 8. Expression of AF GWAS loci from Human Heart Cell Atlas.

Atlas. Dot plot displaying the mean expression of AF GWAS genes across all cell states identified by the Human Heart Cell Atlas. Top, bars are colored according to the clusters presented in our study (**Figure 6c**). SAN, sinoatrial node; AVN, atrioventricular node; P cell, pacemaker cell; aCM, atrial cardiomyocyte; vCM, ventricular cardiomyocyte; EC, endothelial cell; PC, pericyte; SMC, smooth muscle cell; FB, cardiac fibroblast; meso,

mesothelial cell (epicardial cell); Adip, adipocyte; NC, neural cell; NK, natural killer cell; Mo, monocyte; MP, macrophage; DC, dendritic cell; Neut, neutrophil.